

Document downloaded from:

<http://hdl.handle.net/10251/182309>

This paper must be cited as:

Khorami, M.; Navarro-Gregori, J.; Serna Ros, P. (2020). Experimental methodology on the serviceability behaviour of reinforced ultra-high performance fibre reinforced concrete tensile elements. STRAIN. 56(5):1-13. <https://doi.org/10.1111/str.12361>



The final publication is available at

<https://doi.org/10.1111/str.12361>

Copyright Blackwell Publishing

Additional Information

EXPERIMENTAL METHODOLOGY ON THE SERVICEABILITY BEHAVIOR OF REINFORCED UHPFRC TENSILE ELEMENTS

M. Khorami*^{1,2}, J. Navarro-Gregori¹ & P. Serna¹

1: Institute of Science and Concrete Technology, ICITECH, Universitat Politècnica de València, València, 46022, Spain.

2: Universidad UTE, Facultad de Arquitectura y Urbanismo, Calle Rumipamba s/n y Bourgeois, Quito, Ecuador

Corresponding Author: Majid Khorami, ICITECH, Av. dels Tarongers, 4D, 46022, Valencia, Spain.
Email address: makho2@doctor.upv.es Tel: +34-655080022

Abstract

Design codes include Serviceability Limit States (SLS) provisions for stress, crack and deflection control in concrete structures, which may limit the structural design. When drawing on reinforced ultra-high performance fiber reinforced concrete (R-UHPFRC), the process of cracking differs significantly from traditional concretes. Thus, it remains unclear whether the traditional provisions are applicable to R-UHPFRC or should be reviewed. Uniaxial tensile tie test is an excellent option to analyze and review these criteria. This work proposes a novel test methodology to study the behavior of R-UHPFRC under serviceability conditions, which lets the study of the global and local deformation behavior by using different measurement equipment. Two different types of R-UHPFRC ties with variant fibre content were tested. The global average tensile stress-strain curve, cracking behavior, number and width of cracks were obtained. Promising preliminary results admitted that this methodology can be useful to propose design criteria of R-UHPFRC under SLS.

Keywords

design criteria, R-UHPFRC, serviceability, SLS requirements, test method, tie.

1 Introduction

The addition of fibers in concrete as reinforcement in the matrix improves post-cracking tensile behavior, energy dissipation capacity, and proper crack distribution. Hence, investigating the tensile properties of ultra-high performance fiber-reinforced concrete (UHPFRC) as a new alternative material for construction is needed. In recent decades, research on this field has increased. From a structural design point of view for UHPFRC, the design criteria, such as crack width limitation and allowable deformation, for serviceability limit state (SLS) may be different from that of conventional concrete; however, studying these requirements is necessary.

Many studies have analyzed the mechanical properties and behavior of conventional concrete and UHPFRC, and have covered various mechanical properties, including shear and flexural behavior, or durability and permeability of concrete among others. A large number of studies were conducted to examine the tensile behavior of fiber concrete without rebar reinforcement^[1-4].

Given that almost all structural elements include steel rebar reinforcement, the mechanical properties of ultra-high performance concrete by using short steel fibers and rebar reinforcement

should be evaluated to increase the structural applications of UHPFRC. High compression strength and improved ductility due to the addition of short steel fibers and well-bonded property between the UHPFRC and the reinforcing bar have of reinforcing bar, and rebar's cover.

The tensile force is generally applied to bars coming out from the specimen's ends. The influence of reinforcement ratio and specimen's shape on cracking distribution was studied by Sasaki et al.^[5], and their results showed that the crack distribution of R-UHPFRC could be increased by decreasing the amount of reinforcement. The experimental result reported by Kunieda et al.^[6], Leutbecher and Fehling^[7] supported the latter inference. An experimental study conducted by Rimkus and Gribniak^[8] considered the influence of the distribution of reinforcing rebar on cracking behavior and crack distance. A particular device that could apply uniform tensile force to all rebars was needed to perform this experiment because of the rebar arrangement and presence of more than one rebar on the specimen's ends. Hence, studies on the distribution of rebar reinforcing effect are limited due to the need for special devices when conducting experimental tests. Therefore, researchers must follow the tensile tie test by only using single rebar reinforcement.

Considering the average crack width, this value is generally acquired from the average amount achieved by dividing the element elongation by the number of cracks. Monitoring the deformation's tie in small distances (local deformation) is logically preferred to increase measurement accuracy. Makita and Brühwiler^[9] installed five displacement transducers (DTs) with a 50 mm lengths on one side of the concrete specimen that achieved consecutive zone deformations at a local scale, and two 250 mm-long LVDTs with their lengths equal to the central part of the specimen; these transducers were used to obtain the global deformation in the uniaxial tensile tie test. Sasaki et al.^[5] also considered the same method when installing twelve 100 mm-long DTs on top of the R-UHPFRC tensile tie in measuring crack opening displacements.

The other method to measure the local deformation of tensile tie is using the digital image correlation technique (DIC) for monitoring the crack propagation and strain distribution at the concrete surface of the tensile tie^[8, 10]. Since DIC is a powerful and useful tool to crack detection and measurement, but this technique cannot express the actual cracking and deformation behaviors because only one side of the tensile element is under monitoring. By contrast, carrying out this method would result in difficulties because of possible movements out of the longitudinal axis. In addition, due to having a large length for the reinforced tensile element, it is needed to set the camera at a long-distance of the specimen losing the image quality. Hence, the identification of the microcracks could be challenging. However, investigating the local tension deformations is necessary to understand the cracking behavior of R-UHPFRC effectively. In the proposed test method, a demountable mechanical strain gauge (DEMEC) with 5 cm distance and measurement accuracy of $\pm 1 \mu\text{m}$ was used.

This study proposed a test method to carry out the uniaxial tensile test for reinforcement UHPFRC ties. The proposed test method was easy to carry out and prepare compared with other techniques without the need for special or complicated equipment. The aim of this work was studying the cracking behavior of R-UHPFRC tensile ties and verifying that for serviceability analysis of R-UHPFRC tensile tie the tension stiffening phenomenon by considering crack formation and crack stabilization, that is used for conventional concrete ties, can be applied, or on the contrary, it is necessary to provide a different approach by considering the micro cracking branch of UHPFRC for this analysis. The results, such as global stress-strain of the tensile tie, local deformations measured via DEMEC equipment, and average crack width were obtained.

The proposed test method could be used to consider the design requirements of UHPFRC under serviceability conditions.

2 Research significance

Defining the design requirements for UHPFRC under SLS was not strongly considered in codes. The uniaxial tensile test is an experimental method that investigates these requirements. Performing a direct tensile test on reinforced concrete specimens and applying tensile force to concrete specimens are difficult tasks. This work provided a simple testing method for exploring the behavior of R-UHPFRC under the uniaxial tension loads in order to analyze the interaction effect between the UHPFRC matrix and the reinforcement. The proposed experimental methodology was easy to perform, used specimens easy to produce in a lab, and the analysis of the experimental results was simple. The proposed method could analyze the deformation behavior of R-UHPFRC tensile elements under SLS conditions by using different types of measurement equipment.

3 Test methodology

3.1 Test setup

3.1.1 Main frame

In this experimental test, a structural frame was necessary in applying the tension force to the R-UHPFRC specimen. The system test should be able to support the maximum force that could be applied to specimens during the test procedure. The system was designed as a horizontal structure for the easy installation of measurement equipment that allows suitable access to the front and back sides of the specimen. The main structure was composed of two plates joined with four rectangular steel tube sections. The distance between two plates was 2000 mm. The plate's dimension was 320 mm × 320 mm with 50 mm-thick. Connector elements were designed to support compression reactions. The elastic buckling capacity was also considered. A 6 mm-thick tube section with 60 × 60 mm size was used based on the allowable stress design for the four connector elements. The st37 (steel material type) was used for all frame members. Figs. 1 and 2 show the details of the main frame.

3.1.2 Force transfer and connection systems

A primary challenge when conducting a uniaxial tensile tie test is the transfer of tensile force or application of displacements from devices to the end rebars of the specimen; hence, different methods were proposed by researchers. Some authors^[7, 11-13] used a jaw system by clamping both rebar ends to connect the concrete specimen to a hydraulic jack device and apply displacement on both ends. Sasaki et al.^[5] used a 22 mm-thick steel plate at each end of the specimen to transfer the tensile force to the specimen. Four rebars were used to ensure sufficient bonding between the plates and UHPFRC. These rebars were welded to the plate and penetrated the UHPFRC tie. On the outside, a screw type reinforcing bar with a 29 mm diameter was welded to apply and transfer the tensile force from devices to the specimen. This connection method is rarely used by researchers due to its difficulties, such as the welding process, special performing details, and possible out-of-plane plate deformation.

Makita and Brühwiler^[9] presented a method to explore the fatigue behavior of UHPFRC reinforced by steel rebars. In this technique for loading and unloading the specimen, a 2 mm-thick aluminum plate was used and guided by epoxy resin to both surfaces of the specimen. These plates were part of the strengthening element. Two U-shaped jaws were used on both sides of the

specimens. A fraction force was produced by applying lateral force at the jaw, and the tensile force could transfer to the specimen. This method was unsuitable for specimens with large section sizes due to low fraction capacity. Amin et al.^[14] used a large section size for SFRC tensile ties with screw-type reinforcing bars at $\text{Ø}20$ and $\text{Ø}28$ mm. The screwed reinforcement was directly connected to the universal joint machine. This technique made it easy to cast, install, and connect the specimen to devices. However, the probability of failure at the end zone is high due to the yielding fracture of rebar considering the different stiffnesses between the bare bar and the end part of the specimen where concrete and reinforcement exist. The spherical hinge joint is another technique used by Rimkus et al.^[10]. In this method, the mechanical anchorage joint is used, and the specimen is connected to machine transfer force devices via the spherical hinge. Notably, the joint detail and method must avoid the fracture by using the yielding mechanism of the bare rebar and end parts of the tensile tie.

The direct tensile test was generally performed by directly applying tension force to the rebar. The rebar should be located exactly along the tie longitudinal axis and pass from the center of the cross-section of the tie element. The hydraulic jack was installed on the left side of the frame, and the movement of the interior cylinder caused displacement at the end border of the hydraulic jack. This test was carried out by using the deformation control method.

The hydraulic jack should be designed as a circular tube with a longitudinal hole to transfer the cylinder's displacement to the specimen. This form helps the steel bar to pass through the interior hole and transfer end border movements of the hydraulic jack to the specimen located inside the frame (see Fig. 2 segment #7).

Given that this investigation focused on SLS of R-UHPFRC, hence it was not needed to achieve the specimen fracture. The applied force value was dependent on the specimen's cross-section and reinforcement diameter. Hence, the steel bar was designed by using a high-strength steel material with $f_y=1000$ MPa and the achieved rebar diameter was 20 mm to support the 200 kN tension force. The hydraulic jack's length was 800 mm; thus, the chosen length for the steel bar that passed through the hydraulic jack was 1000 mm. The same 600 mm-long steel bar was used on the right side of the frame. A screw thread was designed on both extremes of the steel rebars to connect and fix the rebar to the frame with the anchorage and washer at the back side of the right plate and end border of the hydraulic jack (Fig. 2). Another side of these steel rebars was embedded with a circular bearing to connect the jaw system.

A primary challenge in conducting the direct tensile test was the connection system in fixing the reinforced concrete element to the transfer force device. As previously mentioned, common methods, such as the wedge-shaped clamp, spherical hinge connection, and end welded to steel anchor plates, were used by researchers. Such systems and methods need special preparation techniques and exhibit difficulties.

The proposed connection system in this research included two-piece steel jaws with 2 mm-high indented corrugations. Each segment was symmetric with the other segment and assembled by using six bolts with a diameter of 13 mm. Indentations that occurred on the rebar body produced sufficient friction force to transfer the tensile force to the specimen by tightening the bolts. Jaw details are provided in Fig. 3b.

Bolts ($\text{Ø}25$ mm) were placed at both ends of the jaws and allowed the steel jaw to be connected to the bars through the steel rod end bearing. This connecting system displayed a hinge behavior and avoided any bending or twisting on the specimen ends (Fig. 3d).

3.2 Materials and specimens

In this experimental research were considered for two types of UHPFRC to evaluate the proposed direct tensile test method and compare the measurement parameters obtained by the test. The dosage of steel fibers for the first (C1) and second (C2) mix designs were 160 and 80 kg/m³, respectively. The length and diameter of applied steel fibers in this study were 13 and 0.2 mm, respectively, and their tensile strength was more than 2000 MPa. Table 1 lists the proposed mixed design.

The procedure was initiated by mixing the dry materials in the mixing chamber for 1 minute to combine all the components well. Water and superplasticizer were added, and the concrete was mixed for approximately 10 minutes until a visible flow was achieved. After the concrete started to flow, steel fibers were added, and the mixing procedure continued for 5 minutes.

The cross-section dimensions usually depend on the machine capacity and reinforcement ratio used for the specimen. Tiberti et al.^[13] and Berbaridi P^[11] tested a wide range of RC and SFRC tensile ties by using seven different square section dimensions (50, 80, 100, 120, 150, 180, and 200 mm) and three different rebar diameters (Ø10, Ø20, and Ø30 mm) to evaluate the crack behavior of ties at SLS. Previous studies^[15-17] have demonstrated that section shape, dimension section, and distribution of reinforcements are significant parameters on the deformation behavior of tensile reinforced ties. Sigrist and Rauch^[12] used large dimensions, such as 110, 160, and 170 mm, for tie square sections and examined the UHPFRC tensile tie reinforced with high-strength steel and conventional steel rebar to investigate the deformation behavior. The obtained experimental results indicated that the stress–strain characteristic and steel rebar type had a significant effect on deformation behavior and the failure mechanism.

In this experimental study, the R-UHPRC tensile tie elements had a prismatic shape. The element length was 1000 ± 2 mm, and its cross-section was a square with 100 mm × 100 mm size. The 1450 mm-long steel reinforcement rebar with Ø12 mm used for all specimens. The nominal yield stress was 522 MPa and Young's modulus was 200 GPa. During the manufacturing procedure, an attempt was made to locate the rebar exactly in the center section to avoid eccentricity and bending effects. Given the different axial stiffnesses at the end of the specimen (the region with and without concrete), two 45 cm-long rebars were used in the external region of the specimen and penetrated 22.5 cm into the concrete specimen to prevent the main bar from yielding and failing on both ends without concrete (Fig. 4). The reinforcement bars were welded at a length of 3–5 cm to the main bar to ensure that no pull-out would occur. The width of indented corrugations located inside the jaw was set to 50 mm to place the three rebars. The test zone was in the center part of the member where only one rebar existed.

The average compression strength values of UHPFRC were 157.73 and 152.41 MPa for concrete types C1 and C2, and the average Young's modulus values obtained by using 150X300 mm cylindrical specimens were 48.53 and 46.49 GPa, respectively. Tensile properties of UHPFRC were obtained by an inverse analysis method developed by López et al.^[18]. For that, prismatic specimens (500X100X100 mm) were tested under four-point bending test. Table 2 provides the constitutive parameters for each specimen and concrete type. In this table (E) is elastic modulus, (f_t) cracking strength, (ϵ_t) strain at cracking strength, ($f_{t,u}$) tensile strength, ($\epsilon_{t,u}$) strain at tensile strength, (w_d) crack opening at change of slope, and (w_0) intersection of the first line of the bilinear σ_w to the w axis.

3.3 Instrumentation

Relevant data from the experimental tensile test should be obtained to study the tensile behavior of R-UHPFRC and evaluate the required design parameters under serviceability conditions. These data reflected the specimen's tensile average stress-strain relationship, average tensile stress in the concrete matrix and reinforcement, cracking behavior, and crack width.

3.3.1 Global and local deformation measurement

In this study, the behavior of the member was studied at the global and local levels. Displacement transducers (DTs) were used to investigate the global behavior. The average value of deformations recorded by DTs was used for rebar deformation by assuming that surface deformations of concrete with steel rebar reinforcement were equal. However, Rimkus and Gribniak^[8] considered this method for investigating the cover effect on reinforced tensile tie with conventional concrete and found that a significant difference existed between the average deformation of the concrete surface and the rebar. The local behavior was evaluated by using demountable mechanical gauges (DEMEC). On both sides of the concrete specimen, four 35 cm-long DTs were utilized to obtain the total tensile elongation of the element (Fig. 5). For local level measurement, #16 DEMEC steel discs were installed at a 1 cm distance from the upper and lower edges on each specimen edge. DEMEC discs were installed on the front and back faces of the element by following the required space for DEMEC machine measurement. Thus, the DTs were installed on the same surface but on top of the concrete specimen by using small plates and hard glue.

3.3.2 Force measurement

The specimens were tested under manually displacement control at a rate about of 0.5 mm/min. The load cell was used to measure the force values located at the right side of the frame behind the plate. The steel bar with 20 mm diameter was connected to the jaw and passed through the hole of the plate where the anchorage and washer were fixed. The applied displacement from the hydraulic jack on the left side of the frame transferred from the steel rebar to the specimen. The tension force in the steel bar caused a compression reaction force between the anchorage and the right plate where an electronic load cell was located. Fig. 3a illustrates the details and position of the cell force.

3.4 Procedure

This experiment was carried out in two stages. The first determined the tension stress-strain relationship of the specimen in the global level. For this purpose, the applied tension force value was measured via load cell and then the rebar tension stress was calculated. Rebar deformation was obtained by using the surface concrete deformation measured by the DTs at the right and left side of specimen. With regard to DTs location and distance from the center of the section, sectional analysis was used, and the rebar elongation (in the center of the section) was obtained via the linear regression method. The average of tension stress-strain relationship obtained for right and left side of specimen was used as a global specimen behavior. The local deformations were obtained by using the DEMEC equipment. The second stage obtained the cracking parameters of specimens and measured the number of cracks to calculate the average crack width. After attaching the DEMEC discs on the front and back surfaces, the specimen was placed inside the jaw and fixed by tightening the six bolts. This process was conducted in a zigzag manner to uniformly distribute the force caused by the tightening of bolts. A specimen axis was installed

along the jaw centerline to avoid applying any bending or torsion to the specimen ends. Before applying the force, the distance between DEMEC discs was measured. This distance will be used to calculate the relative elongation after the force was applied to the element. Force application should be stopped because the measuring process of DEMEC equipment is time-consuming, and the amount of specimen elongation should be measured in every stopped force level. The applied force for all specimens was stopped in the value strains of 0.03%, 0.05%, 0.10%, 0.15%, 0.5%, 1%, 1.5%, and 2%. When the distance between DEMEC discs was measured, the force was maintained at a constant level. The first phase of the test was completed as the average element tensile strain reached 2%, and the experiment was stopped. Then, the crack propagation scheme drawn on the specimen's surfaces without unloading the specimen to keep the cracks open. The number of cracks on the upper and lower edges between the DEMEC discs on the specimen's six edges was recorded by wetting the surface with water.

4 Test results and discussion

4.1 Global tensile behavior

In this work, the concrete surface strain monitored by DTs was used to obtain the reinforcement strain, which was located in the center of the tie section. As previously mentioned, four DTs were present in each side of the specimen to record element tensile elongation. A slight difference in the force-displacement diagrams obtained by each DT was observed. This characteristic likely occurred due to the asymmetric cracks that appeared on the specimen's cross-section and very small rotations. Fig. 6 illustrates the average force-displacement curves recorded by four DTs on the left and right sides of specimen T10-12-C1-1 as an example.

Figs. 7a and 7b present the results obtained for the two categories of R-UHPFRC by two different concrete types (C1 and C2) and three specimens for each category. These diagrams demonstrated the global stress-strain relationship of tie elements. The stress expressed in this diagram was shown as the equivalent steel stress, which was obtained by dividing the total tensile force by the area of the reinforced steel.

A significant difference was observed for the first cracking strength by increasing the fiber content in the concrete matrix. The first cracking strength for tie type C1 and C2 were 533 and 426 MPa, respectively. Note that in this study, the difference between the fiber contents was twofold. The average stiffness values in the elastic branch obtained by the three test samples of concrete types C1 and C2 were 6800 and 3123 GPa, respectively. In the elastic region due to force equilibrium and strain compatibility was not observed crack in the matrix. This outcome indicated that the applied force was shared between the rebar and UHPFRC. For fibre activation, a small opening at the crack was necessary to allow slip between the matrix and the fiber. At the first cracking, a small portion of the rebar will lose bond from the concrete. If this process continues, then an increasing number of microcracks along the element will develop^[8]. It can be seen that after the first cracking a significant reduction in stiffness happened and the member response curve of ties by concrete type C1 moved forward parallel to the bare steel response, while for ties by concrete type C2 the tension response curve became diminish and response line has a small curve similar to the tension behavior for conventional concrete or FRC ties.

In addition, another result, which can be obtained from the general tensile response of R-UHPFRC tensile element, is the tension stiffening effect. The tension stiffening refers to the ability of the concrete to carrying the tension between cracks. This phenomenon has an effect on member stiffness, and it is essential for determining the serviceability deflection, and crack widths^[19]. The

tension stiffening effect should be included in the analysis to predict member behavior by employing an appropriate model. Sturm, A et al^[20] proposed a tension stiffening model for FRC and UHPFRC by considering the strain-softening and strain-hardening with an allowance for the long-term creep and shrinkage effects of the concrete. The obtained tension stiffening effect for concrete type C1 and C2 is presented in Fig. 8. The R-UHPFRC specimens exhibit a quasi-constant tension stiffening effect (refer to the horizontal branch of the curve), even at high-tension strain rates closed to 2%. Moreover, the increment of the UHPFRC concrete contribution due to the increasing fiber content can be seen. It is important to outline that the fiber collaboration in the UHPFRC tensile elements has two fundamental effects: (a) fibers provide a significant residual post-cracking strength, and (b) a state of stabilized microcracking is generated thanks to the bond between the UHPFRC matrix and the fibers improving ductility behavior even for UHPFRC with only 80 kg/m³.

The stress–strain diagrams, and the tension stiffening response obtained by the proposed method demonstrated the efficiency of this method in carrying out future research and studying the tensile behavior of R-UHPFRC structural elements.

4.2 Local tensile behavior

The measured local deformations obtained by the DEMEC equipment helped evaluate the strain distribution along the tensile element length and its variation in different force stages. The same evaluation was initiated^[21] by installing DEMEC discs on the four cross-sectional corners in a symmetric form. The average elongation measured by the four corner points was used to obtain the steel rebar strain in the center of the section. Figs. 9 and 10 show the results obtained for two different concrete types of tensile R-UHPFRC ties.

Certain crack amounts of the tie element and crack opening differed with the other parts due to the stochastic nature of concrete cracking. Thus, the local strain distribution diagrams along the element length varied.

By comparing the local deformation results obtained for the two types of concrete, the ties that include 80 kg/m³ fibers demonstrated a significant difference with those with a fiber dosage of 160 kg/m³. Consequently, the amount of fiber content in tensile R-UHPFRC tie elements exhibited an influence on deformation behavior, and their design parameters under SLS conditions. Thus, the proposed measurement method could be used to investigate these parameters.

The results of the proposed measurement method showed that this method is able to capture the maximum tensile strains along the specimen, its position, and its variation. Using together the experimental data obtained by DEMECs and DTs leads to having a potential experimental methodology for studying the serviceability behavior of R-UHPFRC.

4.3 Cracking behavior (propagation of cracks and crack width)

Cracking behavior parameters, such as width and crack spacing, were influenced by the reinforcement ratio and rebar diameter for conventional concrete. The fiber content exhibited a significant effect on this behavior^[22]. The observed first cracks at the concrete surface were very small (called microcracks). The crack width was increased with increasing tensile force. At the

end of the test and after obtaining the tensile strain of 2‰, the number of cracks between the DEMEC discs installed on the specimen's six edges was recorded by wetting the surface with water. The average crack width was calculated by dividing the total achieved elongation at the 2‰ tensile strain (total elongation recorded from the right and left sides by DTs) by the number of cracks. The number of cracks in each edge was slightly different due to the inhomogeneous cracking manner. Table 3 lists the number of cracks on each side of the specimen and the average crack width of two different R-UHPFRC ties as examples. No cracks were clearly observed due to the rough surface created on the specimen that did not come into contact with the steel mold.

The medium crack width for the R-UHPFRC tensile tie with 80 and 160 kg/m³ fiber content was obtained 0.054 and 0.026 mm, respectively. The main crack space was obtained by dividing the entire length of the measurement zone by average number of cracks. The crack spacing of concrete type C1 and C2 was 10.16 and 17.44 mm, respectively. This difference emphasized the clear influence of fiber volume content on crack width and serviceability behavior. Figs. 11a and 11b illustrate the crack propagation for the prior specimens. The crack pattern obtained for the two types of UHPFRC showed that substantial microcracks (with minor width) occurred in the tie with high fiber content and the high fiber content caused the cracking process by mines distance between them. Considering the difference of cracks amounts and crack distance for two types of ties, the microcracking effect can be taken into account for tension stiffening analysis.

5 Summary and conclusions

In this research, a new test method is proposed to carry out the uniaxial tensile test for R-UHPFRC tie. This method can evaluate the tensile behavior of R-UHPFRC under serviceability conditions, and help understand the deformation and cracking behaviors of tie elements. The experimental test was designed with two stages; in the first stage, defined the global tension behavior, and in the second stage obtained the local deformation behavior along the member length in small distances. Six specimens with two different fiber contents were examined.

The experimental study showed that the increase in fiber volume content of concrete has a significant influence on first cracking strength. In this study fiber content for concrete type C1 = 80 kg/m³ and C2 = 160 kg/m³. The local deformation behavior in small segments along the member length was analyzed. The result showed that R-UHPFRC tensile ties with concrete type C2 had more significant local tensile strain than those with C1 concrete type due to the enlarged crack width. The fiber volume content had an important influence on the cracking and serviceability behaviors of R-UHPFRC.

The obtained results of the proposed test method demonstrated the suitability of this test method in carrying out the uniaxial R-UHPFRC tensile test, and in analyzing the interaction effect between the UHPFRC matrix and the reinforcement. Consequently, the proposed test methodology is appropriate for future studies on serviceability design criteria for R-UHPFRC.

Acknowledgments

This work was supported by the State Research Agency of Spain and formed a part of Project "BIA2016-78460-C3-1-R".

References

- [1] Y. Kusumawardaningsih, E. Fehling, M. Ismail, A. A. M. Aboubakr, *Procedia Engineering* **2015**, *125*, 1081-1086.
- [2] A. E. Naaman, H.-W. Reinhardt, *Materials and structures* **2006**, *39*, 547-555.

- [3] S. H. Park, D. J. Kim, G. S. Ryu, K. T. Koh, *Cement and Concrete Composites* **2012**, *34*, 172-184.
- [4] K. Wille, S. El-Tawil, A. E. Naaman, *Cement and Concrete Composites* **2014**, *48*, 53-66.
- [5] K. Sasaki, R. Mori, M. Kunieda, in *International Conference on Strain-Hardening Cement-Based Composites*, Springer, **2017**, pp. 502-508.
- [6] M. Kunieda, M. Hussein, N. Ueda, H. Nakamura, *Journal of Advanced Concrete Technology* **2010**, *8*, 49-57.
- [7] T. Leutbecher, E. Fehling, *ACI Structural Journal* **2012**, *109*.
- [8] A. Rimkus, V. Gribniak, *Construction and Building Materials* **2017**, *148*, 49-61.
- [9] T. Makita, E. Brühwiler, *International Journal of Fatigue* **2014**, *59*, 145-152.
- [10] A. Rimkus, R. Jakstaite, R. Kupliauskas, L. Torres, V. Gribniak, *Procedia Engineering* **2017**, *172*, 930-936.
- [11] M. E. Bernardi P, Minelli F, Sirico A and Tiberti G, in *Computational Modelling of Concrete Structures - Proceedings of EURO-C 2014, Vol. 2*, Taylor and Francis - Balkema, **2014**, pp. 883-892.
- [12] V. Sigrist, M. Rauch, *Tailor Made Concrete Structures-Walraven & Stoelhorst (eds)* **2008**, 405-410.
- [13] G. Tiberti, F. Minelli, G. A. Plizzari, F. J. Vecchio, *Cement and Concrete composites* **2014**, *45*, 176-185.
- [14] A. Amin, S. J. Foster, M. Watts, *Magazine of Concrete Research* **2015**, *68*, 339-352.
- [15] I. Vilanova, L. Torres, M. Baena, G. Kaklauskas, V. Gribniak, *Engineering Structures* **2014**, *79*, 390-400.
- [16] N. J. Carino, N. J. Carino, *Prediction of cracking in reinforced concrete structures*, US Department of Commerce, National Institute of Standards and Technology, **1995**.
- [17] V. Gribniak, A. Rimkus, L. Torres, R. Jakstaite, *Structural Concrete* **2017**, *18*, 634-647.
- [18] J. Á. López, P. Serna, J. Navarro-Gregori, E. Camacho, *Materials and Structures* **2015**, *48*, 3703-3718.
- [19] A. Sturm, P. Visintin, D. Oehlers, *Journal of Structural Engineering* **2019**, *145*, 04019138.
- [20] A. Sturm, P. Visintin, D. Oehlers, R. Seracino, *Journal of Structural Engineering* **2018**, *144*, 04018122.
- [21] T. Pfyl, P. Marti, *Versuche an stahlfaserverstärkten Stahlbetonelementen, Vol. 268*, ETH Zurich, **2001**.
- [22] J. R. Deluce, F. J. Vecchio, *ACI Structural Journal* **2013**, *110*.

TABLE 1 UHPFRC mixture design.

| Component | Content (kg/m³) |
|------------------------------------|-----------------------------------|
| Cement I 42.5 R/SR | 800 |
| Silica fume 940 D Elkem UD | 175 |
| Silica flour U-S500 | 225 |
| Fine sand 0.5 mm | 302 |
| Medium sand 0.6–1.2 mm | 565 |
| Water | 160 |
| Superplasticizer, Viscocrete 20 HE | 30 |
| Fiber | 160 |

TABLE 2 Main characteristics of R-UHPFRC ties

| Material code | Fiber dosage (kg/m ³) | Tie code | E (GPa) | f _t (MPa) | ε _t (‰) | f _{t,u} (MPa) | ε _{t,u} (‰) | w _d (mm) | w ₀ (mm) |
|---------------|-----------------------------------|-------------|---------|----------------------|--------------------|------------------------|----------------------|---------------------|---------------------|
| C1 | 160 | T10-12-C1-1 | 52.73 | 7.91 | 0.15 | 6.52 | 2.11 | 2.27 | 3.40 |
| | 160 | T10-12-C1-2 | 49.66 | 8.94 | 0.18 | 8.03 | 4.04 | 1.90 | 2.84 |
| | 160 | T10-12-C1-3 | 51.50 | 10.30 | 0.20 | 9.58 | 5.09 | 1.99 | 2.99 |
| C2 | 80 | T10-12-C2-1 | 62.62 | 7.40 | 0.11 | 4.87 | 3.32 | 2.20 | 3.30 |
| | 80 | T10-12-C2-2 | 54.64 | 7.58 | 0.13 | 4.69 | 2.94 | 3.98 | 5.97 |
| | 80 | T10-12-C2-3 | 62.06 | 7.44 | 0.12 | 4.27 | 2.90 | 2.46 | 3.69 |

TABLE 3 Average number of cracks recorded between DEMEC discs and the average width of cracks for specimens T10-12-C1-1 and T10-12-C1-1

| | | T10-12-C1-1 (Force level value = 122.82) | | | T10-12-C2-1 (Force level value = 110.72) | | |
|--------------------------|-------|---|--------------------------|-----------------------|---|--------------------------|------------------------------------|
| Measurement surface side | Edges | Total Number of Cracks | Achieved Elongation (mm) | Mean Crack Width (mm) | Total Number of Cracks | Achieved Elongation (mm) | Mean Crack Width (μm) |
| Top side | Edge1 | 78 | 1.890 | 0.0242 | 39 | 2.299 | 0.0589 |
| | Edge2 | 78 | 1.890 | 0.0242 | 39 | 2.299 | 0.0589 |
| Front Side | Edge1 | 77 | 1.890 | 0.0245 | 50 | 2.299 | 0.0459 |
| | Edge2 | 64 | 1.890 | 0.0295 | 47 | 2.299 | 0.0489 |
| Back Side | Edge1 | 87 | 1.890 | 0.0217 | 45 | 2.299 | 0.0510 |
| | Edge2 | 59 | 1.890 | 0.0320 | 38 | 2.299 | 0.0605 |
| | | | Mean | 0.026 | | Mean | 0.054 |

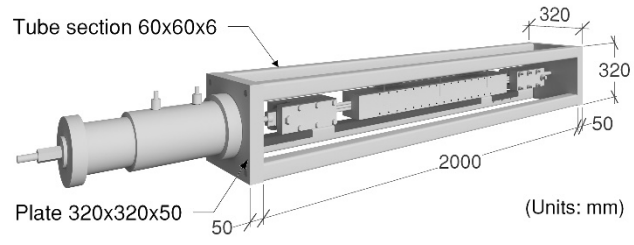
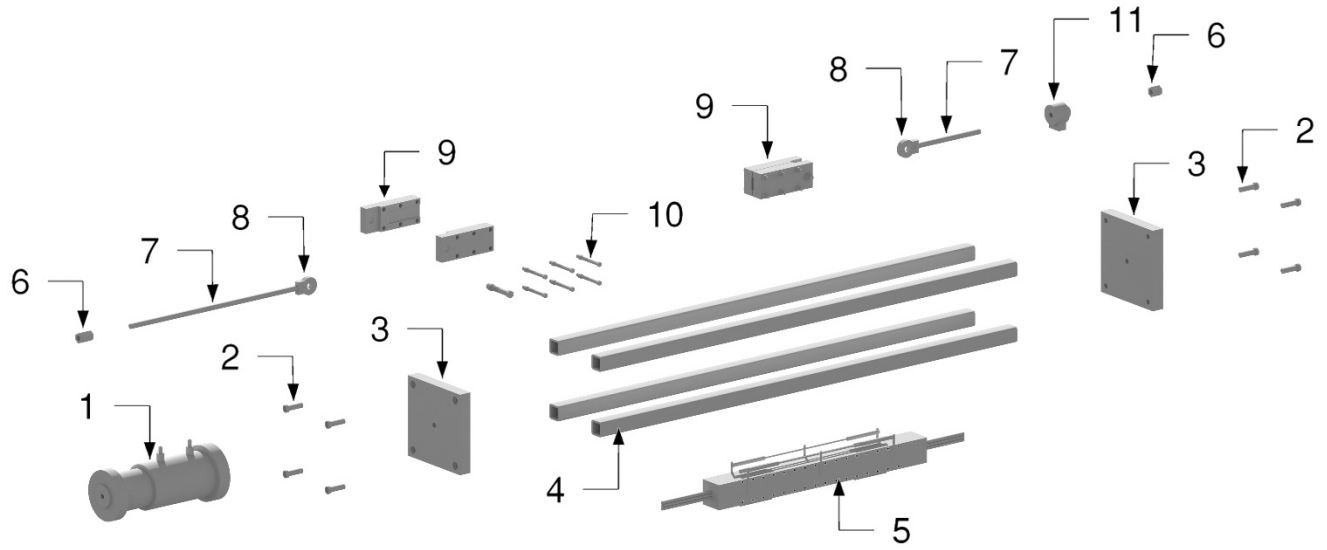


FIGURE 1 Main frame and installed concrete specimen.



Test set-up assembly parts

- | | |
|-----------------------------|---------------------------|
| 1.- Hydraulic jack | 7.- Steel rebar Ø20 mm |
| 2.- Bolt Ø20 mm | 8.- Steel rod end bearing |
| 3.- Plate 320 x 320 x 50 mm | 9.- Steel Jaw |
| 4.- Tube section 60 x 60 mm | 10.- Bolts Ø13 mm |
| 5.- Concrete specimen | 11.- Cell-force |
| 6.- Anchorage | (Units: mm) |

FIGURE 2 Test setup of assembly parts.

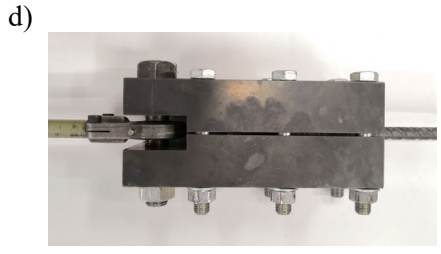
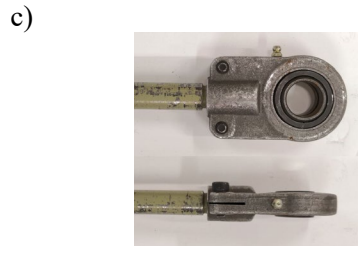
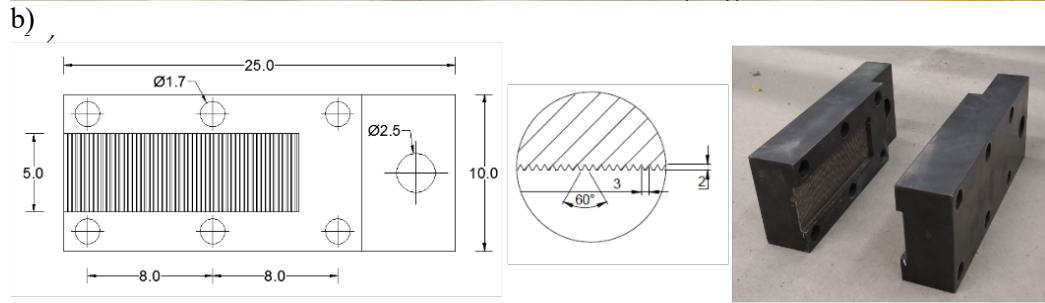
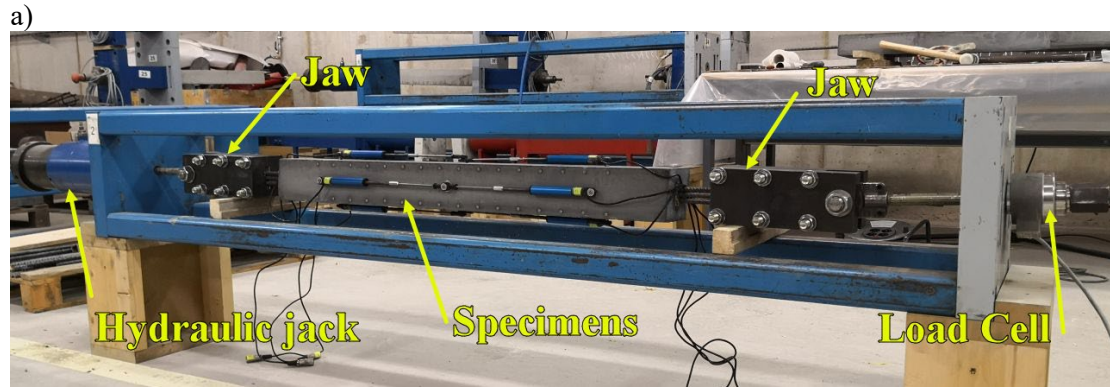


FIGURE 3 a) Tensile test equipment. b) Jaw details. c) Rod end bearing. d) Assembled jaw connection.

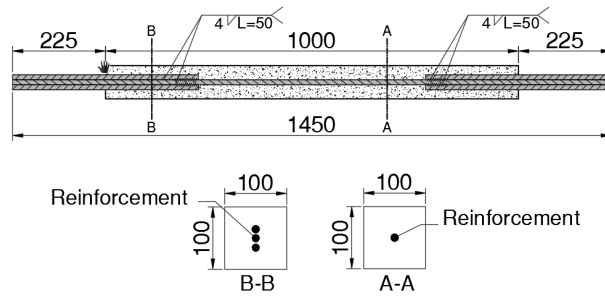


FIGURE 4 Specimen reinforcement details (units in mm).

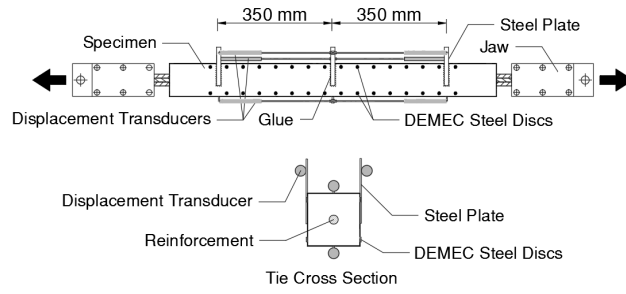


FIGURE 5 Measurement equipment: positions of DTs and DEMEC points along the element.

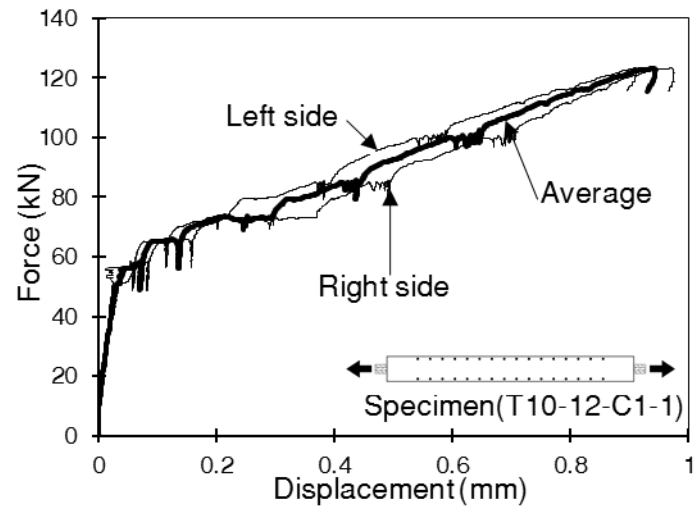


FIGURE 6 Displacement–force relationship of specimen T10-12-C1-1.

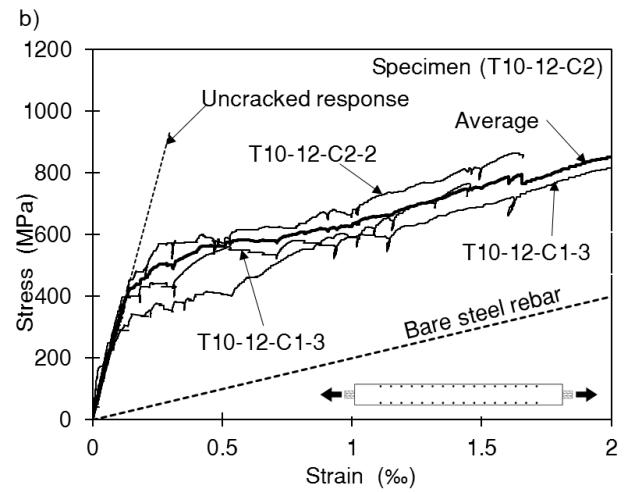
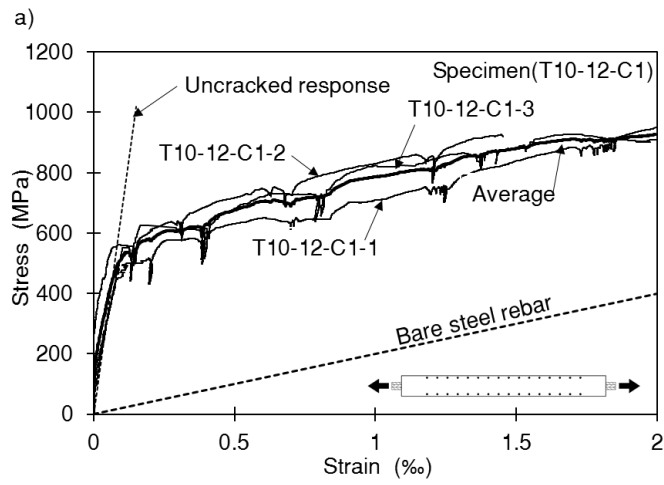


FIGURE 7 Tensile stress–strain diagram: a) concrete type C1 (fiber dosage = 160 kg/m^3); b) concrete type C2 (fiber dosage = 80 kg/m^3)

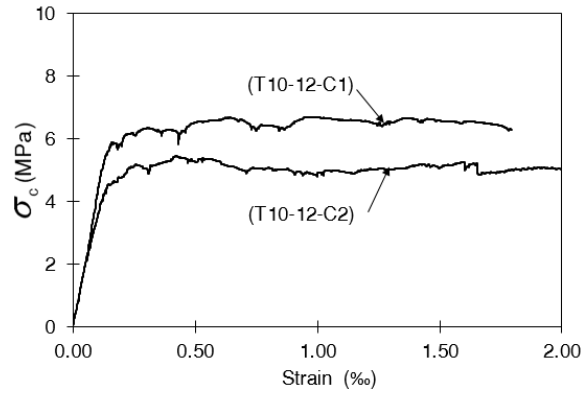


FIGURE 8 Tension stiffening response for concrete type C1, and C2

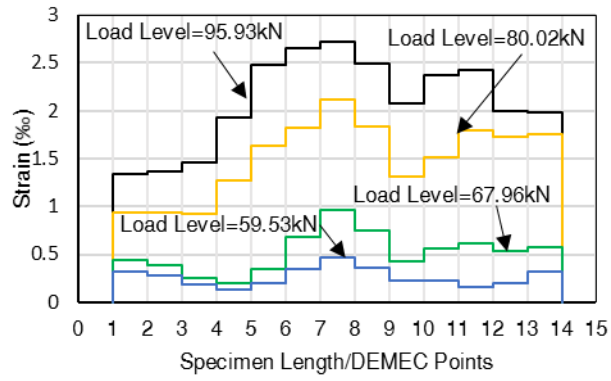


FIGURE 9 Strain distribution along the tie length of R-UHPFRC tensile tie #T10-12-C1-1

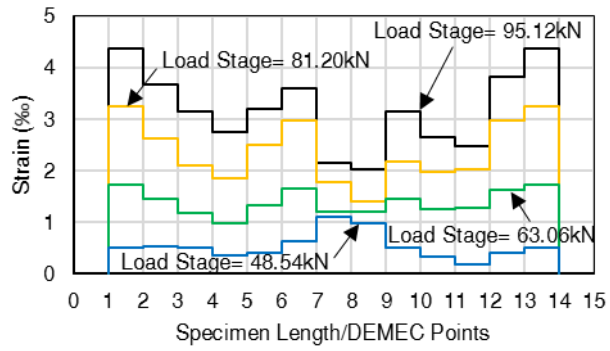


FIGURE 10 Strain distribution along the tie length of R-UHPFRC tensile tie #T10-12-C2-1

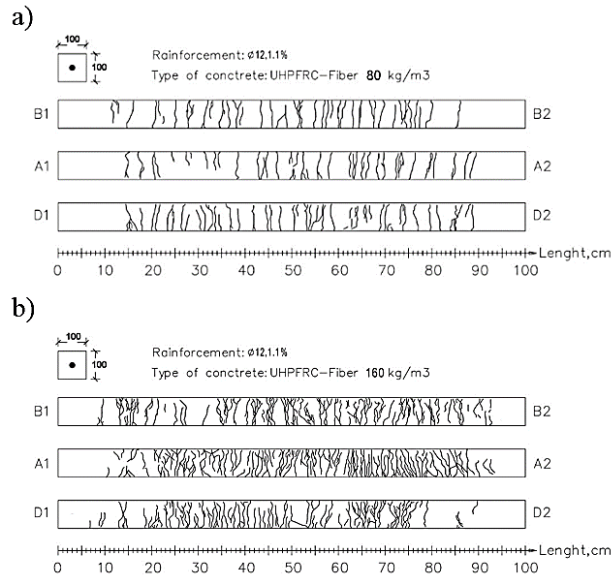


FIGURE 11 Crack pattern of specimens a) T10-12-C1-1 and b) T10-12-C2-1